

基于日光诱导叶绿素荧光的北半球森林物候研究

周 稳¹ 迟永刚¹ 周 蕾^{1,2*}

¹浙江师范大学地理与环境科学学院, 浙江金华 321004; ²中国科学院地理科学与资源研究所生态系统网络观测与估算重点实验室, 北京 100101

摘 要 植被物候是反映植被生长规律的重要指标, 对气候的反馈具有重要意义。日光诱导叶绿素荧光(SIF)通过复杂的能量耗散机制与光合作用相关, 提供了从空间直接探测大范围植被物候的可能性。为了探究气候变化背景下SIF反演不同森林类型物候的适用性, 该文以北半球35个全球通量网(FLUXNET)森林站点为研究对象, 利用2007–2014年SIF值和通量数据总初级生产力(GPP)通过双逻辑生长模型和动态阈值法来估算3种典型森林类型的物候, 并采用相关性分析等方法评价SIF在不同森林类型物候估算时的差异性。主要结果为: (1) SIF对生长季开始时间(SOS)的估算精度高于生长季结束时间(EOS); (2) SIF更能够准确地估算混交林(MF)的SOS, 但是不能精确追踪落叶阔叶林(DBF)和常绿针叶林(ENF)的SOS; (3)春季季前短波辐射是驱动SOS的主要气候因素。综上, 建议在将来的研究中将SIF数据与其他遥感指数整合, 应用于不同植物类型的物候监测。

关键词 植被物候; 北方森林; 日光诱导叶绿素荧光; 气候变化; 短波辐射

周稳, 迟永刚, 周蕾 (2021). 基于日光诱导叶绿素荧光的北半球森林物候研究. 植物生态学报, 45, 00-00. DOI: 10.17521/cjpe.2020.0376

Vegetation phenology in the Northern Hemisphere based on the solar-induced chlorophyll fluorescence

ZHOU Wen¹, CHI Yong-Gang¹, and ZHOU Lei^{1,2*}

¹College of Geography and Environmental Sciences, Zhejiang Normal University, Jinhua, Zhejiang 321004, China; and ²Key Laboratory of Ecosystem Network Observation and Modelling, Institute of Geographic Sciences and Natural Resources Research, Chinese Academy of Sciences, Beijing 100101, China

Abstract

Aims Vegetation phenology is an important indicator to reflect the stages of vegetation growth, which is of great significance to the feedback to climate. Solar-induced chlorophyll fluorescence (SIF) is a by-product of photosynthesis, which provides the possibility to directly detect vegetation phenology at the global scale. In order to reveal the accuracy of phenology estimated by SIF of different forest types, we estimated phenology of three forest types in the Northern Hemisphere.

Methods Based on 35 eddy flux tower sites in the Northern Hemisphere during the period of 2007–2014, we estimated phenology of three typical forest types using SIF value and gross primary production (GPP) by double logistic growth model and dynamic threshold. Correlation analysis was used to evaluate the different potential of SIF in estimating phenology of different forest types.

Important findings Results showed that: (1) SIF was more suitable to estimate the timing of the start of growing season (SOS) than the timing of the end of growing seasons (EOS). (2) SOS based on SIF had the highest correlation with SOS based on GPP in mixed forests (MF). However, the SOS of deciduous broadleaf forest (DBF) and Evergreen Needleleaf forest (ENF) could not be accurately tracked by SIF value. (3) The pre-season shortwave radiation (SR) was the primarily environmental factor of SOS.

Key words vegetation phenology; northern forest; solar-induced chlorophyll fluorescence; climate change; shortwave radiation

Zhou W, Chi YG, Zhou L (2021). Vegetation phenology in the Northern Hemisphere based on the solar-induced chlorophyll fluorescence. *Chinese Journal of Plant Ecology*, 45, 00-00. DOI: 10.17521/cjpe.2020.0376

植被物候能够反映植物在一年中的生长发育规律(Piao *et al.*, 2019)。生长季开始时间(SOS)和生长

季结束时间(EOS)描述了植被生命周期的发育、活跃生长和衰老阶段(周蕾等, 2020)。准确的物候监测

收稿日期Received: 2020-11-18 接受日期Accepted: 2021-01-11

基金项目: 国家重点研发计划(2017YFB0504000)和国家自然科学基金(41871084和31400393)。Supported by the National Key R&D Program of China (2017YFB0504000), and the National Natural Science Foundation of China (41871084 and 31400393).

* 通信作者Corresponding author (zhoulei@zjnu.cn)

对于估算陆地与大气之间的碳水交换具有重要意义。近年来,遥感技术成为估算大尺度植被物候的有效手段(代武君等, 2020)。

日光诱导叶绿素荧光(SIF)是有效光合辐射中小部分辐射的再发射,延伸到近红外波段,具有红光(690 nm左右)和近红外(740 nm左右)两个波峰(Jeong *et al.*, 2017)。在理论上, SIF通过复杂的能量耗散机制与光合作用相关联(Guanter *et al.*, 2014; Zhang *et al.*, 2016), 而且SIF产品对云和大气散射不敏感(Piao *et al.*, 2019)。因此, SIF数据为探测大尺度植被物候提供了一种可靠的方法(Bertani *et al.*, 2017; Li *et al.*, 2018; 刘啸添等, 2018)。然而, SIF数据与光合作用之间的联系会随着植被类型的不同而发生变化。Li等(2018)通过对8种植被的比较发现, 相对于常绿针叶林和灌木林, SIF更适用于估算温带混交林和落叶阔叶林的物候。SIF在估算不同森林物候时所表现出的差异性能力可能与植被的冠层结构(Guan *et al.*, 2016)、生理特性(Sun *et al.*, 2017)、环境变化(Lee *et al.*, 2015)以及景观异质性(Zhang *et al.*, 2020)密切相关。因此, 需要从全球尺度比较SIF对不同森林类型物候的追踪能力。

植物物候发生的时间与环境因素息息相关(Yang *et al.*, 2020a)。气温是影响植被生长周期的重要环境因素。一般来说, 气温升高会促进叶片提前发育和推迟衰老, 然而气温降低则会推迟叶片发育和加快叶片衰老(Piao *et al.*, 2007)。植被物候也会受到降水的影响, 特别是在干旱和半干旱地区(Shen *et al.*, 2019)。充足的水分会促进叶片发育的提前(Jin *et al.*, 2019), 而延缓植被叶片的衰老(Liu *et al.*, 2016a; Yuan *et al.*, 2020)。此外, 辐射也是引起物候发生变化的重要气候因子, 一般来说春季辐射的增强会导致生长季开始时间的提前, 而冬季辐射的增强会导致春季物候的推迟(Yang *et al.*, 2020b)。因此, 理解气候因素对植被物候的驱动和调控机制, 以及理解植物对气候系统的反馈具有重要意义。

森林是陆地生物圈的主体, 在调节全球碳水循环和能量平衡方面发挥着至关重要的作用(方精云, 2000; Huang *et al.*, 2020)。本研究从全球通量网(FLUXNET) 2015数据集中选取了北半球35个森林站点, 通过总初级生产力(GPP)和SIF值分别估算2007–2014年不同森林类型的物候, 分析SIF在估算植被物候方面的潜力, 比较SIF追踪不同森林类型

物候的能力, 进而探索植被物候的环境影响机制。

1 材料和方法

1.1 研究站点

本研究选取了FLUXNET中北半球35个森林站点作为研究对象。站点选取原则为: (1)选取SIF和GPP数据都超过3年的站点; (2)选取SIF和GPP数据每年的填充率都在80%以上的站点(Xu *et al.*, 2019b)。研究站点包括19个常绿针叶林(ENF)、11个落叶阔叶林(DBF)和5个混交林(MF)站点。

1.2 SIF数据

本研究采用搭载在MetOp-A卫星上的GOME-2反演得到日尺度SIF数据(Köhler *et al.*, 2015) (<https://avdc.gsfc.nasa.gov/index.php>)。该产品是基于主成分分析从740 nm左右波段范围提取的8天最大值, 空间分辨率为 $0.5^\circ \times 0.5^\circ$ (Joiner *et al.*, 2013)。本研究通过站点的坐标提取出2007–2014年的日尺度SIF数据。

1.3 GPP数据和气象数据

本研究采用FLUXNET 2015数据集(<https://fluxnet.org/data/fluxnet2015-dataset/>)中日尺度GPP。该数据是由涡度相关测量技术直接观测得到净生态系统交换量(NEE), 然后将NEE拆分为GPP和生态系统呼吸量(ER)(Yang *et al.*, 2017)。本研究首先将SIF值和GPP平均到8天并计算相关性。其次为了验证SIF追踪物候的精度, 本研究使用GPP作为对照数据, 和SIF使用同样的方法反演物候(Lu *et al.*, 2018b; Wang *et al.*, 2019b, 2020)。

本研究的气温(TA_F)、降水(P_F)和辐射(SW_IN_F)采用和GPP时间范围一致的FLUXNET 2015数据集。本研究采用季前环境因子与物候之间的相关性探索气候条件的变化对物候的影响(Yuan *et al.*, 2020)。首先分别获取物候前1–4个月的环境因子, 并与物候进行偏相关性分析, 最佳季前长度即环境因子与物候之间偏相关系数最大的时段(Jeong *et al.*, 2011; Liu *et al.*, 2016a)。为了减少数据的偏差, 本研究对超过5年数据的29个站点分别采用最佳季前长度的环境因子和基于SIF的生长季开始时间做相关性分析(Xu *et al.*, 2019a)。

1.4 物候确定方法

部分原始数据存在着质量差以及缺失的现象, 造成物候观测的不确定性(章钊颖等, 2019)。本研究

采用既能保护数据关键点, 又能抵抗植被参数噪声的三次样条插值法校准和插补GPP和SIF数据(Liu *et al.*, 2017)(图1)。

本研究通过双逻辑生长模型(公式(1))拟合SIF和GPP时间序列数据确定植被的物候(Chang *et al.*, 2019; Wang *et al.*, 2019a), 物候学的双逻辑生长模型有效地解释了在生长季节观察到的大部分冠层覆盖的时间模式。由二阶导数曲线检测到的物候能够代表大多数植被物候(Tan *et al.*, 2011)。SOS和EOS分别对应拟合曲线的二阶导数开始和结束时两个极大值相对应的日期(Wang *et al.*, 2019a)(图2)。

$$g(t) = a_1 + \frac{a_2}{1 + \exp(-b_1 * (t - d_1))} - \frac{a_3}{1 + \exp(-b_2 * (t - d_2))} \quad (1)$$

式中, $g(t)$ 为 t 时刻的SIF值或者GPP, a_1 为背景植被参数, a_2 为初夏植被参数峰值, a_3 为夏末植被参数峰值, b_1 和 d_1 分别控制与叶发育阶段相对应的时间序列增加部分的时间和斜率, b_2 和 d_2 分别控制与叶衰老阶段相对应的时间序列递减部分的时间和斜率。

为了验证双逻辑生长模型的结果, 我们同时使用动态阈值确定物候(Jeong *et al.*, 2011; Shen *et al.*, 2020)。首先用六项式(公式(2))拟合GPP和SIF值年度曲线, 然后对拟合后的GPP和SIF值归一化, 最后将0.2设置为阈值追踪物候(Jeong *et al.*, 2017, Wang *et al.*, 2019a)

$$y(t) = \alpha + \alpha_1 \times t + \alpha_2 \times t^2 + \dots + \alpha_n \times t^n, n = 6 \quad (2)$$

式中, $y(t)$ 为 t 时刻的SIF值或者GPP, $\alpha - \alpha_n$ 是拟合参数。

$$Ratio_{day}(t) = (y(t) - y_{min}) / (y_{max} - y_{min}) \quad (3)$$

式中, $y(t)$ 是拟合后的SIF值或者GPP, y_{max} 和 y_{min} 是拟合后一年中最大和最小的SIF值或者GPP。

2 结果和分析

2.1 SIF值和GPP的相关性

研究结果显示3种森林的SIF值和GPP的时间序列曲线均呈现单峰形态的季节性动态(图3), 3种森林的时间轨迹在春季能够重合, 然而落叶阔叶林和常绿针叶林的时间轨迹在结束时差异较大。SIF值与GPP之间都存在显著的线性相关性(图4)。其中SIF值与GPP在混交林的相关性最高($R^2 = 0.72$, $p < 0.05$), 其次是常绿针叶林($R^2 = 0.65$, $p < 0.05$), 而落叶阔叶林中SIF值与GPP相关系数最低($R^2 = 0.59$, $p < 0.05$)。

2.2 基于SIF和基于GPP的物候对比分析

研究结果显示通过双逻辑生长模型和动态阈值两种不同的方法, SIF均能捕捉森林的SOS, 但对各种森林类型表现出不同的能力(图5)。SIF对混交林的SOS表现出较强的追踪能力, 通过双逻辑生长模型和动态阈值基于SIF值和GPP估算出的SOS的相关性分别为 $R^2 = 0.48$ 和 $R^2 = 0.21$ ($p < 0.05$)。在落叶阔叶林, 通过动态阈值法基于SIF值和GPP追踪的SOS的相关性($R^2 = 0.20$, $p < 0.05$)大于通过双逻辑生长模型追踪的两种SOS的相关性($R^2 = 0.13$, $p < 0.05$)。而在常绿针叶林, 通过双逻辑生长模型追踪的两种SOS的相关性($R^2 = 0.19$, $p < 0.05$)大于通过动态阈值法追踪的两种SOS的相关性($R^2 = 0.14$, $p < 0.05$)。另外, SIF值通过双逻辑生长模型估算的混交林SOS ((93 ± 28) DOY)也比较接近基于GPP估算的SOS ((101 ± 26) DOY), 其偏差值为(-8 ± 21) d (图6)。SIF值通过双逻辑生长模型估算的常绿针叶林和落叶阔叶林的SOS和基于GPP估算的SOS的偏差值分别为(-5 ± 35)和(-26 ± 31) d。

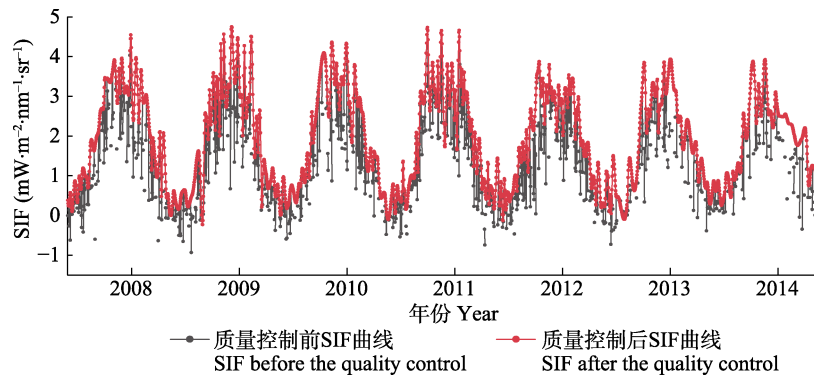


图1 原始日光诱导叶绿素荧光(SIF)曲线与经过质量控制后的SIF曲线对比图。

Fig. 1 Comparison between time series curves of solar-induced chlorophyll fluorescence (SIF) before and after the quality control.

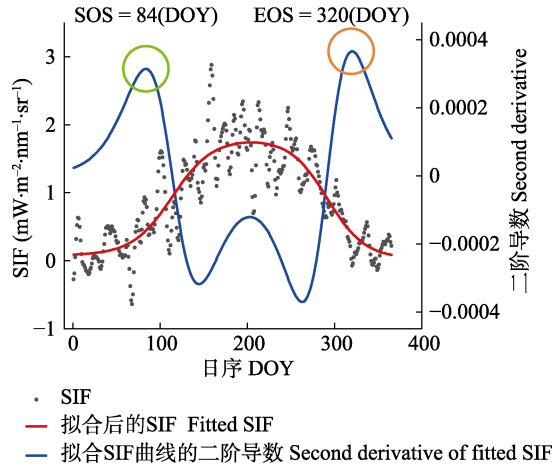


图2 日光诱导叶绿素荧光(SIF)通过双逻辑生长模型拟合物候曲线示意图。生长季开始时间(SOS)即绿色圆圈对应日期,生长季结束时间(EOS)即橙色圆圈对应日期。

Fig. 2 An example for determining the phenology based on daily solar-induced chlorophyll fluorescence (SIF) time series using double logistic growth model. Timing of the start of the growing season (SOS) and the end of the growing season (EOS) were plotted by green circle and orange circle. DOY, day of year.

相对于SOS, SIF并不能准确地捕捉到森林的EOS (图5)。SIF只能估算混交林的EOS, 通过动态阈

值法基于SIF值和GPP追踪的EOS的相关性($R^2 = 0.21, p < 0.05$)大于通过双逻辑生长模型追踪的两种EOS的相关性($R^2 = 0.13, p < 0.05$)。然而在常绿针叶林和落叶阔叶林, SIF值反演的EOS和GPP反演的EOS的相关性并不显著($p > 0.05$)。SIF值通过双逻辑生长模型估算的常绿针叶林、落叶阔叶林和混交林的EOS和基于GPP估算的EOS的偏差值分别为(5 ± 40)、(-22 ± 44)和(15 ± 29) d。

2.3 气候因子对基于SIF的SOS的影响

研究结果显示春季季前短波辐射是影响森林SOS的主要气候变量(图7)。其中, 75%的站点受到短波辐射的影响, 而且春季季前短波辐射与SOS呈正相关关系, 相关性为 0.89 ± 0.08 ($p < 0.05$)。SOS受春季季前气温影响的站点占28%, 春季季前辐射与SOS呈正相关关系, 其相关性为 0.89 ± 0.07 ($p < 0.05$)。SOS受春季季前降水影响的站点只有25%, 大部分站点中季前降水与SOS呈现正相关关系, 其相关性为 0.41 ± 0.08 ($p < 0.05$)。

在不同的森林中, 季前短波辐射和SOS之间的

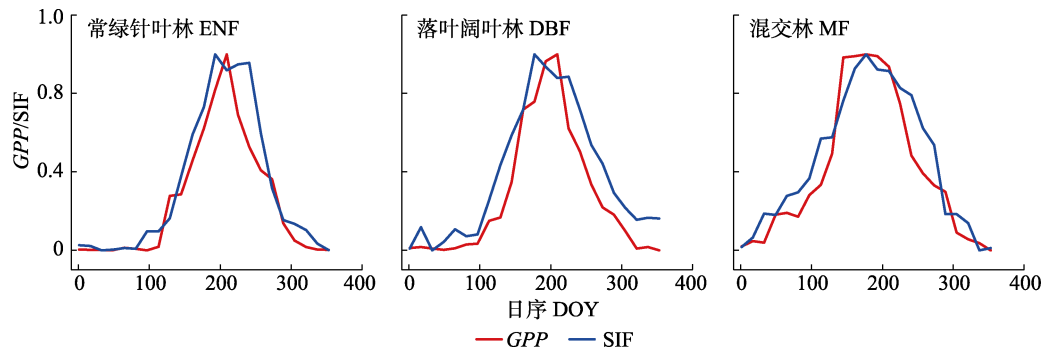


图3 标准化日光诱导叶绿素荧光(SIF)值和总初级生产力(GPP)的季节动态。

Fig. 3 Seasonal trajectories of normalized solar-induced chlorophyll fluorescence (SIF) value and gross primary production (GPP). DBF, deciduous broadleaf forest; ENF, evergreen needleleaf forest; MF, mixed forests. DOY, day of year.

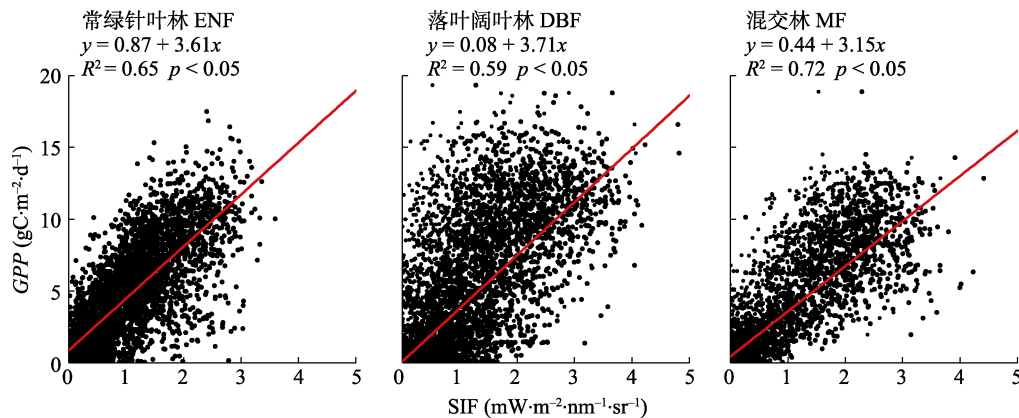


图4 基于8天均值日光诱导叶绿素荧光(SIF)值和总初级生产力(GPP)的相关性。

Fig. 4 Correlations between 8-day solar-induced chlorophyll fluorescence (SIF) value and gross primary production (GPP). DBF, deciduous broadleaf forest; ENF, evergreen needleleaf forest; MF, mixed forests.

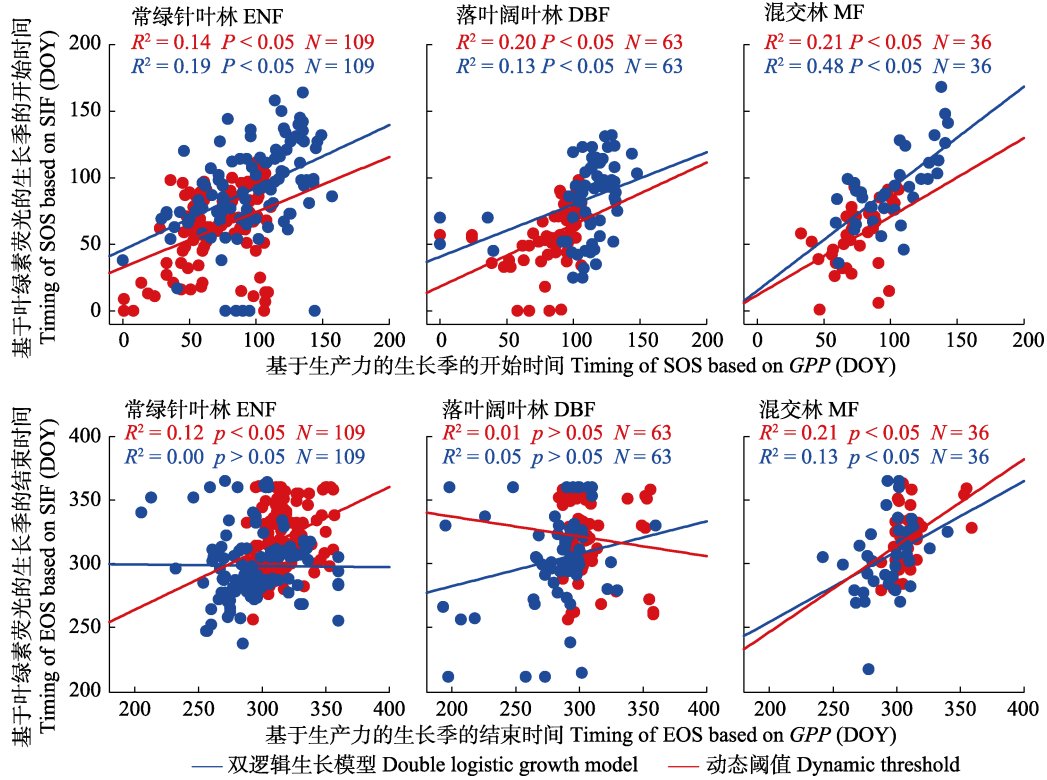


图5 基于日光诱导叶绿素荧光(SIF)值和总初级生产力(GPP)估算的生长季开始时间(SOS)和生长季结束时间(EOS)的关系。DOY, 日序; N, 所有站点的总年份。

Fig. 5 Scatterplots describing the relationship between timing of the start of growing season (SOS) and timing of the end of growing season (EOS) derived from solar-induced chlorophyll fluorescence (SIF) value and gross primary production (GPP). DOY, day of year; N, the years of all sites. DBF, deciduous broadleaf forest; ENF, evergreen needleleaf forest; MF, mixed forests.

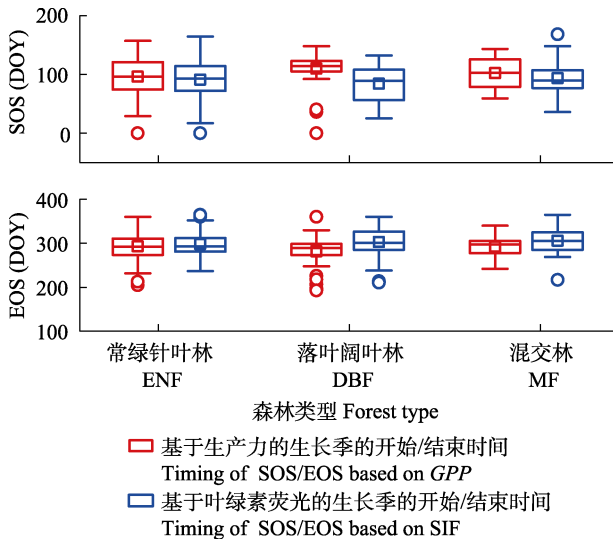


图6 基于日光诱导叶绿素荧光(SIF)值和总初级生产力(GPP)估算的生长季开始时间(SOS)和生长季结束时间(EOS)的分布图。DOY, 日序。

Fig. 6 Distributions of timing of the start of the growing season (SOS) and timing of the end of the growing season (EOS) derived from solar-induced chlorophyll fluorescence (SIF) value and gross primary production (GPP). DBF, deciduous broadleaf forest; ENF, evergreen needleleaf forest; MF, mixed forests. DOY, day of year.

相关性差异不大, 在混交林中, 季前短波辐射与SOS的相关性为 0.83 ± 0.12 ($p < 0.05$), 在落叶阔叶林中, 季前短波辐射与SOS的相关性为 0.92 ± 0.04 ($p < 0.05$), 在常绿针叶林中, 季前短波辐射与SOS的相关性为 0.90 ± 0.09 ($p < 0.05$)。季前气温和降水对不同森林得SOS没有显著的影响。

3 讨论

3.1 SIF对不同森林物候估算的适用性

SIF作为光合作用的副产品, 多项研究表明SIF值与GPP之间几乎呈线性关系(Cui *et al.*, 2017; Frankenberg *et al.*, 2011), 而且在温带和北方森林中SIF值和GPP表现出较强的季节相关性(Yang *et al.*, 2015), 近期的研究表明基于SIF值的物候在不同地区表现出与GPP几乎相同的物候模式(Jeong *et al.*, 2017)。这些结果表明, SIF可以用作大规模物候监测, 从而增进对物候学的理解。

以往有关遥感物候的研究表明, 对于大多数植被类型而言, SOS比EOS更有可能获得高建模精度

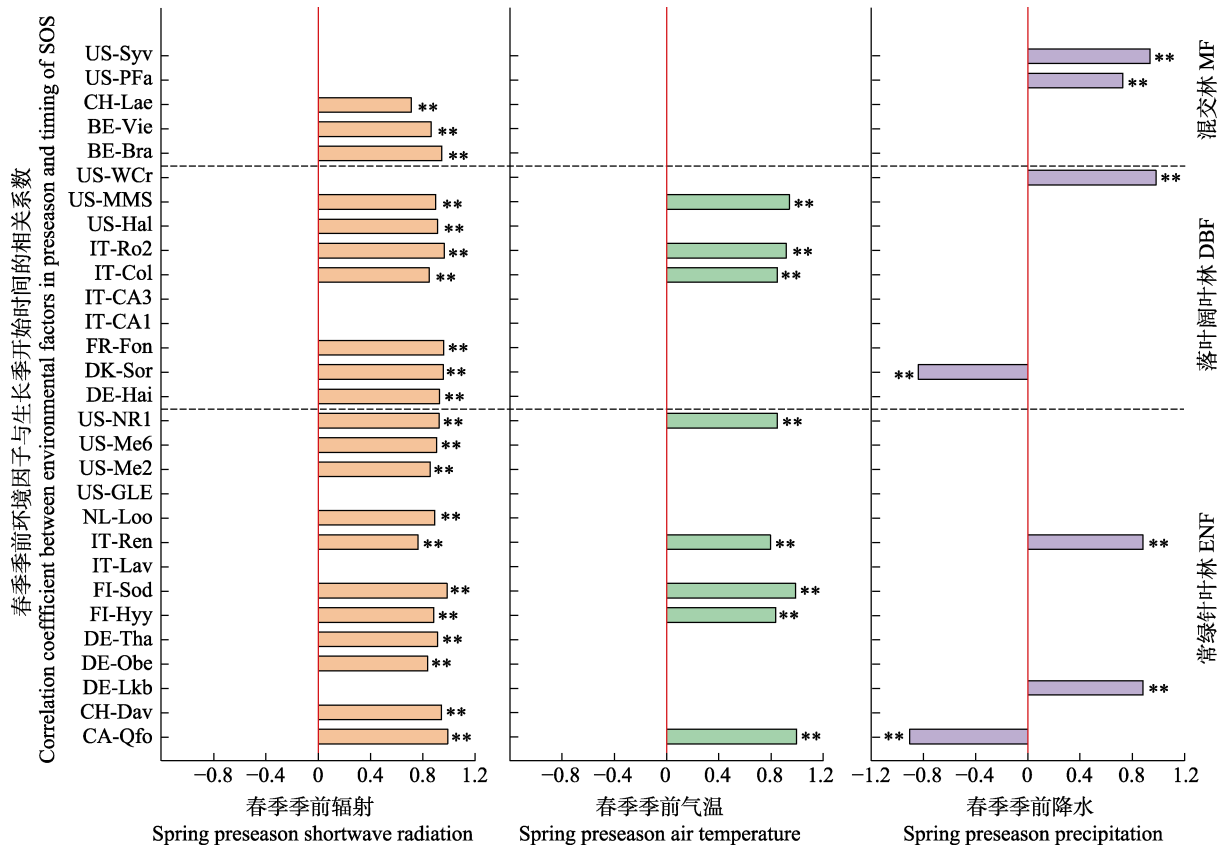


图7 春季季前环境因子(短波辐射、气温、降水)与生长季开始时间(SOS)的相关系数(r)。**, $p < 0.05$ 。纵坐标为FLUXNET中的森林站点名称。

Fig. 7 Correlation coefficient (r) of environmental factors (shortwave radiation, air temperature, precipitation) in pre-season and timing of the start of the growing season (SOS). **, $p < 0.05$. DBF, deciduous broadleaf forest; ENF, evergreen needleleaf forest; MF, mixed forests. The Y-axis represents the forest site name in FLUXNET.

(Wu *et al.*, 2017), 我们同样证实了该观点。在绿化阶段, 植被绿度变化的原因是叶绿素的增加、叶面积的增加以及其他叶片性状的变化, 这些变化与光合作用和呼吸作用有关(Wu *et al.*, 2017)。因此, SIF能够追踪到生长季的开始。但是, 在衰老阶段, 植物的冠层绿度变化和光合作用变化要经历时间更长, 而且变化速度更慢的过程(Liu *et al.*, 2016b)。从而使衰老事件的监测更加困难。

SIF值和GPP的相关性在混交林最高(图4), 同样基于SIF值估算出的混交林的物候更接近于基于GPP估算出的物候(图6)。以往关于北半球中高纬度森林物候的研究同样表明, SIF值和GPP的线性相关性在混交林比常绿针叶林和落叶阔叶林强, 而且基于SIF值的物候在混交林更接近于基于GPP的物候(Lu *et al.*, 2018a)。SIF追踪不同森林物候的差异性可能与冠层结构和景观异质性有关。冠层结构变化对森林的GPP变化有重要的影响, 明显的季节动态使得估算混交林物候相对容易。然而常绿针叶林植被冠

层结构季节性变化较小, GPP的季节动态主要由植被生理变化引起(Chang *et al.*, 2019)。另外, 落叶阔叶林SIF值的误差可能源自景观异质性(He *et al.*, 2017), 当GPP基本为0时, 可能由于林下植被还有信号(Zhang *et al.*, 2020), 或者GOME-2的信噪比产生一些异常值(Köhler *et al.*, 2015), 导致SIF值产生误差, 从而不能准确估算落叶阔叶林的物候。因此, 在全球范围内使用SIF值估算植被物候时, 应考虑SIF对不同植被的适用性。

3.2 基于SIF植被物候的环境驱动机制

季前环境因子广泛应用于物候环境因子的评价中(Jeong *et al.*, 2011; Liu *et al.*, 2016a)。植被的春季物候主要取决于前几个月的环境因子, 北半球季前长度的变化从几周到4个月不等(Shen *et al.*, 2014)。最佳季前长度对应的环境因子对春季物候的影响, 能够体现植被生长季开始时间的环境驱动机制。

季前短波辐射对SOS起主要驱动作用, 其次是季前气温(图7)。随着春季季前辐射和季前气温的增

强, SOS推迟。气温是植物生长的基本需求, 在植物生长发育过程中发挥重要作用(Xie *et al.*, 2015; Liu & Zhang, 2020)。但是绿色植物大部分的能源是经由光合作用从太阳光中得到的, 以往的研究同样表明了辐射对于物候的重要性(管琪卉等, 2019; Inoue *et al.*, 2020)。太阳辐射是地球陆地生态系统演化的主要驱动力, 为光合作用提供了能量(Wilson & Meyers, 2007)。短波辐射在植物活动中起着关键作用, 通过影响乙烯和脱落酸这两种参与芽形成和叶片发育的植物激素, 调节植物内源激素调节的生长和蛋白质生产(Zhong *et al.*, 2012; Singh *et al.*, 2017; Peaucelle *et al.*, 2019)。植被需要一定的冷冻积累才能进入生态休眠阶段, 然而在季节性解冻之前强烈的季前短波辐射会减少冬季的冷冻积累, 从而限制植被的生长(Yang *et al.*, 2020b)。因此, 在研究植被物候的环境驱动机制时, 需要进一步考虑辐射对物候的影响。

3.3 不确定分析

本研究通过站点GPP来验证GOME-2 SIF估算不同森林类型物候的能力, 主要存在空间分辨率方面的不确定性。我们采用的GOME-2 SIF数据空间分辨率较粗($0.5^{\circ} \times 0.5^{\circ}$), 也许在站点尺度上追踪物候存在一定的限制。然而, 已经有研究表明GOME-2 SIF与GPP具有高度的一致性(Zhang *et al.*, 2016), 而且通过GOME-2 SIF估算的物候比归一化植被指数(NDVI)等植被指数估算的物候更为精确(Jeong *et al.*, 2017)。

4 结论

本研究以北半球35个森林站点为研究对象, 采用基于GOME-2 SIF数据以及基于FLUXNET的GPP来估算3种典型森林类型的物候期, 评价SIF值与GPP在拟合物候期时的线性关系, 明确SIF值在估算不同森林类型物候时的潜力。结果表明SIF值可以代替GPP追踪物候, 然而SIF值在估算不同植被类型的物候时具有不同的潜力, 具体体现在SIF数据对常绿针叶林和落叶阔叶林的物候的追踪能力不如对混交林的物候的追踪。并且, SIF值对SOS的追踪比对EOS更为精确。此外, 春季季前短波辐射是驱动SOS的关键因素。因此, 在未来研究中, 可以将SIF数据与其他遥感指数整合, 应用于不同植物功能型的物候估算。

致谢 感谢FLUXNET网站(<https://fluxnet.org/>)提供GPP时间序列以及气象数据和Köhler等反演的SIF数据(<ftp://doidata.gfz-potsdam.de/open/GlobFluo/GOME-2/>)。

参考文献

- Bertani G, Wagner FH, Anderson LO, Aragão LJRS (2017). Chlorophyll fluorescence data reveals climate-related photosynthesis seasonality in Amazonian forests. *Remote Sensing*, 9, 1275. DOI: 10.3390/rs9121275.
- Chang Q, Xiao X, Jiao W, Wu X, Doughty R, Wang J, Du L, Zou Z, Qin Y (2019). Assessing consistency of spring phenology of snow-covered forests as estimated by vegetation indices, gross primary production, and solar-induced chlorophyll fluorescence. *Agricultural and Forest Meteorology*, 275, 305-316.
- Cui T, Sun R, Qiao C (2017). Analyzing the relationship between solar-induced chlorophyll fluorescence and gross primary production using remotely sensed data and model simulation. *International Journal of Earth & Environmental Sciences*, 2, 129. DOI: 10.15344/2456-351X/2017/129.
- Dai WJ, Jin HY, Zhang YH, Zhou ZQ, Liu T (2020). Advances in plant phenology. *Acta Ecologica Sinica*, 40, 6705-6719. [代武君, 金慧颖, 张玉红, 周志强, 刘彤 (2020). 植物物候学研究进展. *生态学报*, 40, 6705-6719.]
- Fang JY (2000). Forest biomass carbon pool of middle and high latitudes in the North Hemisphere is probably much smaller than present estimates. *Acta phytocologica Sinica*, 24, 635-638. [方精云 (2000). 北半球中高纬度的森林碳库可能远小于目前的估算. *植物生态学报*, 24, 635-638.]
- Frankenberg C, Fisher JB, Worden J, Badgley G, Saatchi SS, Lee JE, Toon GC, Butz A, Jung M, Kuze A (2011). New global observations of the terrestrial carbon cycle from GOSAT: patterns of plant fluorescence with gross primary productivity. *Geophysical Research Letters*, 38, L17706. DOI: 10.1029/2011GL048738.
- Guan K, Berry JA, Zhang Y, Joiner J, Guanter L, Badgley G, Lobell DB (2016). Improving the monitoring of crop productivity using spaceborne solar-induced fluorescence. *Global Change Biology*, 22, 716-726.
- Guan QH, Ding MJ, Zhang HM (2019). Spatiotemporal variation of spring phenology in alpine grassland and response to climate changes on the Qinghai-Tibet, China. *Mountain Research*, 37, 639-648. [管琪卉, 丁明军, 张华敏 (2019). 青藏地区高寒草地春季物候时空变化及其对气候变化的响应. *山地学报*, 37, 639-648.]
- Guanter L, Zhang Y, Jung M, Joiner J, Voigt M, Berry JA, Frankenberg C, Huete AR, Zarco-Tejada P, Lee JE, Moran MS, Ponce-Campos G, Beer C, Camps-Valls G, Buchmann N, *et al.* (2014). Global and time-resolved monitor-

- ing of crop photosynthesis with chlorophyll fluorescence. *Proceedings of the National Academy of Sciences of the United States of America*, 111, E1327-E1333.
- He L, Chen JM, Liu J, Mo G, Joiner J (2017). Angular normalization of GOME-2 Sun-induced chlorophyll fluorescence observation as a better proxy of vegetation productivity. *Geophysical Research Letters*, 44, 5691-5699.
- Huang JG, Ma Q, Rossi S, Biondi F, Deslauriers A, Fonti P, Liang E, Mäkinen H, Oberhuber W, Rathgeber CBK, Tognetti R, Trembl V, Yang B, Zhang JL, Antonucci S, *et al.* (2020). Photoperiod and temperature as dominant environmental drivers triggering secondary growth resumption in Northern Hemisphere conifers. *Proceedings of the National Academy of Sciences of the United States of America*, 117, 20645-20652.
- Inoue S, Dang QL, Man R, Tedla B (2020). Photoperiod, [CO₂] and soil moisture interactively affect phenology in trembling aspen: implications to climate change-induced migration. *Environmental and Experimental Botany*, 180, 104269. DOI: 10.1016/j.envexpbot.2020.104269.
- Jeong SJ, Ho CH, Gim HJ, Brown ME (2011). Phenology shifts at start vs. end of growing season in temperate vegetation over the Northern Hemisphere for the period 1982–2008. *Global Change Biology*, 17, 2385-2399.
- Jeong SJ, Schimel D, Frankenberg C, Drewry DT, Fisher JB, Verma M, Berry JA, Lee JE, Joiner J (2017). Application of satellite solar-induced chlorophyll fluorescence to understanding large-scale variations in vegetation phenology and function over northern high latitude forests. *Remote Sensing of Environment*, 190, 178-187.
- Jin H, Jönsson AM, Olsson C, Lindström J, Jönsson P, Eklundh L (2019). New satellite-based estimates show significant trends in spring phenology and complex sensitivities to temperature and precipitation at northern European latitudes. *International Journal of Biometeorology*, 63, 763-775.
- Joiner J, Guanter L, Lindstrot R, Voigt M, Vasilkov AP, Middleton EM, Huemmrich KF, Yoshida Y, Frankenberg C (2013). Global monitoring of terrestrial chlorophyll fluorescence from moderate-spectral-resolution near-infrared satellite measurements: methodology, simulations, and application to GOME-2. *Atmospheric Measurement Techniques*, 6, 2803-2823.
- Köhler P, Guanter L, Joiner J (2015). A linear method for the retrieval of sun-induced chlorophyll fluorescence from GOME-2 and SCIAMACHY data. *Atmospheric Measurement Techniques*, 8, 2589-2608.
- Lee JE, Berry JA, van der Tol C, Yang X, Guanter L, Damm A, Baker I, Frankenberg C (2015). Simulations of chlorophyll fluorescence incorporated into the Community Land Model version 4. *Global Change Biology*, 21, 3469-3477.
- Li X, Xiao J, He B, Altaf Arain M, Beringer J, Desai AR, Emmel C, Hollinger DY, Krasnova A, Mammarella I, Noe SM, Ortiz PS, Rey-Sanchez AC, Rocha AV, Varlagin A (2018). Solar-induced chlorophyll fluorescence is strongly correlated with terrestrial photosynthesis for a wide variety of biomes: first global analysis based on OCO-2 and flux tower observations. *Global Change Biology*, 24, 3990-4008.
- Liu LL, Zhang XY (2020). Effects of temperature variability and extremes on spring phenology across the contiguous United States from 1982 to 2016. *Scientific Reports*, 10, 17952. DOI: 10.1038/s41598-020-74804-4.
- Liu Q, Fu YH, Zhu Z, Liu Y, Liu Z, Huang M, Janssens IA, Piao S (2016a). Delayed autumn phenology in the Northern Hemisphere is related to change in both climate and spring phenology. *Global Change Biology*, 22, 3702-3711.
- Liu RG, Shang R, Liu Y, Lu XL (2017). Global evaluation of gap-filling approaches for seasonal NDVI with considering vegetation growth trajectory, protection of key point, noise resistance and curve stability. *Remote Sensing of Environment*, 189, 164-179.
- Liu XT, Zhou L, Shi H, Wang SQ, Chi YG (2018). Phenological characteristics of temperate coniferous and broad-leaved mixed forests based on multiple remote sensing vegetation indices, chlorophyll fluorescence and CO₂ flux data. *Acta Ecologica Sinica*, 38, 3482-3494. [刘啸添, 周蕾, 石浩, 王绍强, 迟永刚 (2018). 基于多种遥感植被指数、叶绿素荧光与CO₂通量数据的温带针阔混交林物候特征对比分析. *生态学报*, 38, 3482-3494.]
- Liu Y, Wu C, Peng D, Xu S, Gonsamo A, Jassal RS, Altaf Arain M, Lu L, Fang B, Chen JM (2016b). Improved modeling of land surface phenology using MODIS land surface reflectance and temperature at evergreen needleleaf forests of central North America. *Remote Sensing of Environment*, 176, 152-162.
- Lu XC, Cheng X, Li XL, Chen JQ, Sun MM, Ji M, He H, Wang SY, Li S, Tang JW (2018a). Seasonal patterns of canopy photosynthesis captured by remotely sensed sun-induced fluorescence and vegetation indexes in mid-to-high latitude forests: a cross-platform comparison. *Science of the Total Environment*, 644, 439-451.
- Lu XL, Liu ZQ, Zhou YY, Liu YL, An SQ, Tang JW (2018b). Comparison of phenology estimated from reflectance-based indices and solar-induced chlorophyll fluorescence (SIF) observations in a temperate forest using GPP-based phenology as the standard. *Remote Sensing*, 10, 932. DOI: 10.3390/rs10060932.
- Peaucelle M, Janssens IA, Stocker BD, Ferrando AD, Fu YH, Molowny-Horas R, Ciais P, Peñuelas J (2019). Spatial variance of spring phenology in temperate deciduous forests is constrained by background climatic conditions. *Nature Communications*, 10, 5388. DOI: 10.1038/s41467-019-13365-1.
- Piao S, Liu Q, Chen A, Janssens IA, Fu Y, Dai J, Liu L, Lian X,

- Shen M, Zhu X (2019). Plant phenology and global climate change: current progresses and challenges. *Global Change Biology*, 25, 1922-1940.
- Piao SL, Friedlingstein P, Ciais P, Viovy N, Demarty J (2007). Growing season extension and its impact on terrestrial carbon cycle in the Northern Hemisphere over the past 2 decades. *Global Biogeochemical Cycles*, 21, GB3018. DOI: 10.1029/2006GB002888.
- Shen MG, Jiang N, Peng DL, Rao YH, Huang Y, Fu YH, Yang W, Zhu XL, Cao RY, Chen XH, Chen J, Miao CY, Wu CY, Wang T, Liang EY, Tang YH (2020). Can changes in autumn phenology facilitate earlier green-up date of northern vegetation? *Agricultural and Forest Meteorology*, 291, 108077. DOI: 10.1016/j.agrformet.2020.108077.
- Shen MG, Tang YH, Chen J, Yang X, Wang C, Cui XY, Yang YP, Han LJ, Li L, Du JH, Zhang GX, Cong N (2014). Earlier-season vegetation has greater temperature sensitivity of spring phenology in Northern Hemisphere. *PLOS ONE*, 9, e88178. DOI: 10.1371/journal.pone.0088178.
- Shen XJ, Liu BH, Xue ZS, Jiang M, Lu XG, Zhang Q (2019). Spatiotemporal variation in vegetation spring phenology and its response to climate change in freshwater marshes of Northeast China. *Science of the Total Environment*, 666, 1169-1177.
- Singh RK, Svystun T, AlDahmash B, Jönsson AM, Bhalerao RP (2017). Photoperiod- and temperature- mediated control of phenology in trees—A molecular perspective. *New Phytologist*, 213, 511-524.
- Sun Y, Frankenberg C, Wood JD, Schimel DS, Jung M, Guanter L, Drewry DT, Verma M, Porcar-Castell A, Griffiths TJ, Gu L, Magney TS, Köhler P, Evans B, Yuen K (2017). OCO-2 advances photosynthesis observation from space via solar-induced chlorophyll fluorescence. *Science*, 358, eaam5747. DOI: 10.1126/science.aam5747.
- Tan B, Morisette JT, Wolfe RE, Gao F, Ederer GA, Nightingale J, Pedelty JA (2011). An enhanced TIMESAT algorithm for estimating vegetation phenology metrics from MODIS data. *IEEE Journal of Selected Topics in Applied Earth Observations and Remote Sensing*, 4, 361-371.
- Wang F, Chen BZ, Lin XF, Zhang HF (2020). Solar-induced chlorophyll fluorescence as an indicator for determining the end date of the vegetation growing season. *Ecological Indicators*, 109, 105755. DOI: 10.1016/j.ecolind.2019.105755.
- Wang X, Xiao J, Li X, Cheng G, Ma M, Zhu G, Altaf Arain M, Andrew Black T, Jassal RS (2019a). No trends in spring and autumn phenology during the global warming *Hiatus*. *Nature Communications*, 10, 2389. DOI: 10.1038/s41467-019-10235-8.
- Wang XY, Wang T, Liu D, Zhang TT, Xu JF, Cui GS, Lv GT, Huang HB (2019b). Multisatellite analyses of spatiotemporal variability in photosynthetic activity over the Tibetan Plateau. *Journal of Geophysical Research*, 124, 3778-3797.
- Wilson TB, Meyers TP (2007). Determining vegetation indices from solar and photosynthetically active radiation fluxes. *Agricultural and Forest Meteorology*, 144, 160-179.
- Wu C, Peng D, Soudani K, Siebicke L, Gough CM, Altaf Arain M, Bohrer G, Lafleur PM, Peichl M, Gonsamo A, Xu S, Fang B, Ge Q (2017). Land surface phenology derived from normalized difference vegetation index (NDVI) at global FLUXNET sites. *Agricultural and Forest Meteorology*, 233, 171-182.
- Xie YY, Wang XJ, Silander JA (2015). Deciduous forest responses to temperature, precipitation, and drought imply complex climate change impacts. *Proceedings of the National Academy of Sciences of the United States of America*, 112, 13585-13590.
- Xu X, Riley WJ, Koven CD, Jia G (2019a). Heterogeneous spring phenology shifts affected by climate: supportive evidence from two remotely sensed vegetation indices. *Environmental Research Communications*, 1, 091004. DOI: 10.1088/2515-7620/ab3d79.
- Xu XJ, Du HQ, Fan WL, Hu JG, Mao FJ, Dong HJ (2019b). Long-term trend in vegetation gross primary production, phenology and their relationships inferred from the FLUXNET data. *Journal of Environmental Management*, 246, 605-616.
- Yang H, Yang X, Zhang Y, Heskell MA, Lu X, Munger JW, Sun S, Tang J (2017). Chlorophyll fluorescence tracks seasonal variations of photosynthesis from leaf to canopy in a temperate forest. *Global Change Biology*, 23, 2874-2886.
- Yang X, Guo R, Knops JMH, Mei L, Kang F, Zhang T, Guo J (2020a). Shifts in plant phenology induced by environmental changes are small relative to annual phenological variation. *Agricultural and Forest Meteorology*, 294, 108144. DOI: 10.1016/j.agrformet.2020.108144.
- Yang X, Tang J, Mustard JF, Lee JE, Rossini M, Joiner J, Munger JW, Kornfeld A, Richardson AD (2015). Solar-induced chlorophyll fluorescence that correlates with canopy photosynthesis on diurnal and seasonal scales in a temperate deciduous forest. *Geophysical Research Letters*, 42, 2977-2987.
- Yang Y, Wu ZF, Guo L, He HS, Ling YH, Wang L, Zong SW, Na RS, Du HB, Li MH (2020b). Effects of winter chilling vs. spring forcing on the spring phenology of trees in a cold region and a warmer reference region. *Science of the Total Environment*, 725, 138323. DOI: 10.1016/j.scitotenv.2020.138323.
- Yuan HH, Wu CY, Gu CY, Wang XY (2020). Evidence for satellite observed changes in the relative influence of climate indicators on autumn phenology over the Northern Hemisphere. *Global and Planetary Change*, 187, 103131. DOI: 10.1016/j.gloplacha.2020.103131.

- Zhang Y, Guanter L, Berry J, van der Tol C, Yang X, Tang J, Zhang F (2016). Model-based analysis of the relationship between sun-induced chlorophyll fluorescence and gross primary production for remote sensing applications. *Remote Sensing of Environment*, 187, 145-155.
- Zhang ZY, Wang SH, Qiu B, Song L, Zhang YG (2019). Retrieval of Sun-induced chlorophyll fluorescence and advancements in carbon cycle application. *Journal of Remote Sensing*, 23, 37-52. [章钊颖, 王松寒, 邱博, 宋练, 张永光 (2019). 日光诱导叶绿素荧光遥感反演及碳循环应用进展. *遥感学报*, 23, 37-52.]
- Zhang ZY, Zhang YG, Porcar-Castell A, Joiner J, Guanter L, Yang X, Migliavacca M, Ju WM, Sun ZG, Chen SP, Martini D, Zhang Q, Li ZH, Cleverly J, Wang HZ, Goulas Y (2020). Reduction of structural impacts and distinction of photosynthetic pathways in a global estimation of GPP from space-borne solar-induced chlorophyll fluorescence. *Remote Sensing of Environment*, 240, 111722. DOI: 10.1016/j.rse.2020.111722.
- Zhong S, Shi H, Xue C, Wang L, Xi Y, Li J, Quail PH, Deng XW, Guo H (2012). A molecular framework of light-controlled phytohormone action in *Arabidopsis*. *Current Biology*, 22, 1530-1535.
- Zhou L, Chi YG, Liu XT, Dai XQ, Yang FT (2020). Land surface phenology tracked by remotely sensed Sun-induced chlorophyll fluorescence in subtropical evergreen coniferous forests. *Acta Ecologica Sinica*, 40, 4114-4125. [周蕾, 迟永刚, 刘啸添, 戴晓琴, 杨风亭 (2020). 日光诱导叶绿素荧光对亚热带常绿针叶林物候的追踪. *生态学报*, 40, 4114-4125.]

责任编辑: 张金屯 编辑: 赵航